Preparation and Properties of Ethylene Propylene Rubber (EPR)–Clay Nanocomposites Based on Maleic Anhydride-Modified EPR and Organophilic Clay

Naoki Hasegawa, Hirotaka Okamoto, Arimitsu Usuki

Toyota Central Research and Development Laboratories, Inc., 41-1, Nagakute, Aichi, 480-1192, Japan

Received 5 August 2003; accepted 3 February 2004
DOI 10.1002/app.20546
Published online in Wiley InterScience (www.interscience.wiley.com).

ABSTRACT: Ethylene propylene rubber–clay nanocomposites (EPR–CNs) were prepared by melt-compounding maleic anhydride modified EPR (EPR-MA) with organophilic clay, and their properties were examined. Silicate layers of organophilic clay were found to exfoliate and homogeneously disperse into the nanometer level in the nanocomposites by transmission electron microscopy observation. EPR–CNs exhibited higher tensile moduli compared to EPR-MA and composites containing conventional fillers such as carbon black, talc. The storage moduli of EPR–CNs were also higher than those of EPR-MA and the conventional composites. Creep resistances of EPR–CNs were much improved compared for EPR-MA. Degree of swelling in hexadecane was remarkably restricted. Improvement of these properties is caused because dispersed silicate layers have much large interface with the EPR matrix and are thought to strongly restrain the EPR polymer chains. Nanocomposite technology using small amount of silicate layers is useful to improve properties of thermoplastic elastomer. Various kinds of thermoplastic elastomers are expected to be produced by loading of silicate layers with or without conventional fillers. © 2004 Wiley Periodicals, Inc. J Appl Polym Sci 93: 758–764, 2004

Key words: nanocomposites; clay; polyolefins; elastomers

INTRODUCTION

In recent years, organic–inorganic nanocomposites have attracted great interest to researchers because they frequently exhibit unexpected hybrid properties synergistically derived from the two components.[1–7] One of the most promising composite systems would be nanocomposites based on organic polymers and inorganic clay minerals consisting of silicate layers.[4–18] In our previous works, we have synthesized a nylon 6–clay nanocomposite, wherein 1-nm thick silicate layers of clay minerals are dispersed homogeneously.[4] The nylon 6–clay nanocomposites exhibits various superior properties such as high strength, high modulus, high heat resistance compared to nylon 6.[4] Since then, other polymer–clay nanocomposites[5–7] such as polyimide,[8] epoxy resin,[9] polystyrene,[10–13] acrylic polymer,[14] and polypropylene (PP)[15–17] were reported.

Recently, we found that functionarized polyolefins intercalated into the galleries of organophilic clay, and we successfully prepared PP–clay nanocomposites based on maleic anhydride-modified PP and organophilic clay.[15,16] In the PP–clay nanocomposites, the silicate layers of the organophilic clay exfoliate and homogeneously disperse at the nanometer level in the PP matrix similar to nylon 6–clay nanocomposites.[17] This approach, introducing maleic anhydride groups to nonpolar polymer chains, is applicable to other polyolefins such as polyethylene, ethylene propylene rubber (EPR), and ethylene propylene diene methylene linkage rubber (EPDM).[18]

EPR, EPDM, and other soft polyolefins are usually used singly as thermoplastic elastomers and compounded with polymer resins as modifiers. Today they are expected as alternative materials to polyvinyl chloride from an environmental point of view. But there is room for improvement in their properties such as heat resistance, creep resistance, and swelling property. For example, the use of the elastomers for interior materials of housing and automobiles is restricted because they are easily swelled with paraffinic oil. Improvement of these properties makes possible wider use of them, and it can be achieved by the application of clay nanocomposite technology to the elastomers. Because silicate layers disperse much more finely in the polymer matrix and drastically restrain the polymer chain mobility compared for conventional fillers such as glass fiber, carbon black, and talc. In this article, we prepare EPR–clay nanocomposites (EPR–CNs) based on maleic anhydride-modified EPR and organophilic clay and examine their mechanical, creep, and swelling properties.

Correspondence to: N. Hasegawa (e0974@mosk.tytlabs.co.jp).

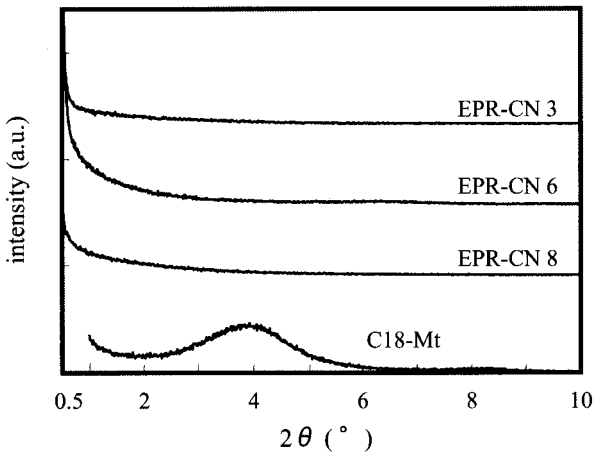

Figure 1 X-ray diffraction patterns of EPR-CNs and C18-Mt.

EXPERIMENTAL

Materials

The materials used for the preparation of the samples are purified montmorillonite (Kunipia-F) from Kunimine Ind. Co., stearylamine from Wako Pure Chemical Co., maleic anhydride-modified EPR (TAFMER MP0610, termed EPR-MA) from Mitsui Chemical Co. The acid value of the EPR-MA is 4.81 mgKOH/g (the amount of the maleic anhydride is 0.42 wt %). The M_n and M_w measured by gel permeation chromatography are 125,000 and 397,000, respectively.

Organophilic clay

Organophilic clay intercalated with stearylammonium was prepared as follows. Sodium montmorillonite (80 g, cation exchange capacity: 119 mEq/100 g) was dispersed into 5000 mL of hot water (about 80°C) by using a homogenizer. Stearylamine (31.1 g, 115 mmol) and conc. HCl (11.5 mL) were dissolved into 2000 mL of hot water. It was poured into the montmorillonite–water solution under vigorous stirring by using a homogenizer for 5 min, producing a white precipitate. The precipitate was collected and washed with hot water three times, and freeze dried to yield an organophilic montmorillonite intercalated with stearylammonuim. It is termed C18-Mt. The interlayer spacing of C18-Mt was 2.20 nm measured by X-ray diffractometry (XRD) (Fig. 1). The inorganic content was 69–71 wt % by measuring the weights before and after burning its organic component.

Preparation of EPR–CNs

EPR–CNs were prepared by melt compounding EPR-MA pellets and C18-Mt powder at 200°C using a twin-screw extruder. The twin-screw extruder was TEX30α-45.5BW from Japan Steal Works Ltd. Its screw length was 1365 mm and its length by diameter (L/D) was 45.5. The obtained strands were pelletized and dried under vacuum at 50°C. The inorganic clay contents of the samples were determined by measuring the weights before and after burning its organic component. The inorganic contents were 2.9 wt % in EPR–CN 3, 6.1 wt % in EPR–CN 6, and 8.3 wt % in EPR–CN 8. For comparison with EPR–CNs, composites containing conventional fillers, carbon black, and talc, were also prepared by melt-compounding in the same manner. The inorganic contents in the EPR–carbon black composites were 5, 15, and 30 wt %, and those in the EPR–talc composites were 5, 10, 20, and 30 wt %.

Evaluation of dispersibility of the clay silicate layers

The dispersion of the silicate layers in EPR–CNs was evaluated by XRD measurements and transmission electron microscopy (TEM) observation. The XRD measurements were performed for films using a Rigaku RAD-B diffractometer with Cu-Kα radiation generated at 30 kV and 30 mA. The films were prepared by compression molding at 150°C. Their thicknesses were 0.4–0.6 mm. The TEM observations were performed for 200-nm thick ultrathin sections cut from a EPR–CN 6 pellet. TEM observations were taken by JEOL-2000EX TEM using an acceleration voltage of 200 kV.

Tensile test

Tensile tests were performed by an Instron Model 4302 at 25°C according to JIS K6251. The crosshead speed was 500 mm/min. Test dumbbells (JIS type 3) were cut from 2-mm thick compression-molded sheets. All measurements were done in four replicates and the value averaged.

Measurement of dynamic moduli

Dynamic viscoelasticity measurements were performed by Iwamoto viscoelastic meter VES-F. The temperature dependence of storage moduli were obtained by sinusoidally vibrating the samples in the tensile mode at 10 Hz. The temperature raising speed was 2°C/min.

Creep test

Creep tests were performed for dumbbells (JIS type 3) under 75 g/cm^2 loading at 100°C. The dumbbells were cut from 2-mm thick compression-molded sheets.

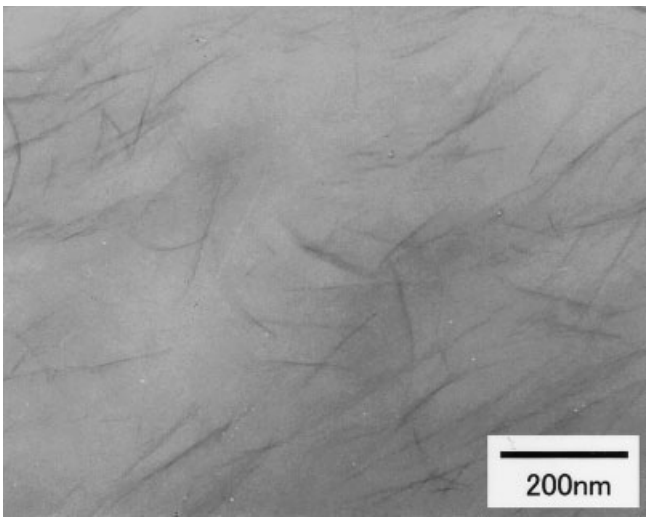

Figure 2 TEM image of EPR-CN 6.

Swelling test

Swelling tests were performed for 10 × 10-mm pieces cut from 2-mm thick compression-molded sheets. The test pieces were soaked in hexadecane at 25°C and measured increments in weight, in length on the plane, and in thickness. Hexadecane is chosen for swelling tests, because hydrocarbons easily swell EPR and hexadecane hardly evaporate at ambient temperature.

RESULTS AND DISCUSSION

Dispersibility of the clay silicate layers

Figure 1 shows the XRD patterns of EPR–CNs and C18-Mt, wherein the peak corresponded to the (001) plane reflections of the layered silicates. There is no peak in the XRD patterns of EPR–CNs; thus, it suggests that there is no regularly stacked layered silicate in EPR–CNs. Figure 2 shows the TEM images of EPR–CN 6, wherein the dark lines are the cross sections of silicate layers of 1-nm thickness. The silicate layers exfoliate and disperse at the nanometer level in EPR–CN 6. With introduction of a small amount of maleic anhydride into EPR polymer chains, the silicate layers disperse into the nanometer level in EPR-MA matrix similar to maleic anhydride modified polypropylene and maleic anhydride modified polyethylene.[18]

Mechanical properties

Representative stress–strain (S-S) curves of the samples are shown in Figure 3. The S-S curve of EPA-MA show typical behavior for an elastomer and has two yield points, the first yield point around 80% strain and the second yield point at the maximum just before the breaking point. In this discussion, the first yield points are defined as the points where the slopes of the S-S curves decease rapidly in less than 100% strain regions. At the first yield point, EPR polymer chains are thought to slip in the process of polymer chain rearrangement. Then the stress increases again by extension of the polymer chains between entanglement points in the larger strain region and EPR-MA is broken around 900% strain after passing through the second yield point. The first yield points in the S-S curves of EPR–CNs are indistinct and become less pronounced with increase of clay content. Strain hardening of EPR–CNs begins in smaller strain region compared to EPR-MA, because rearrangement of the

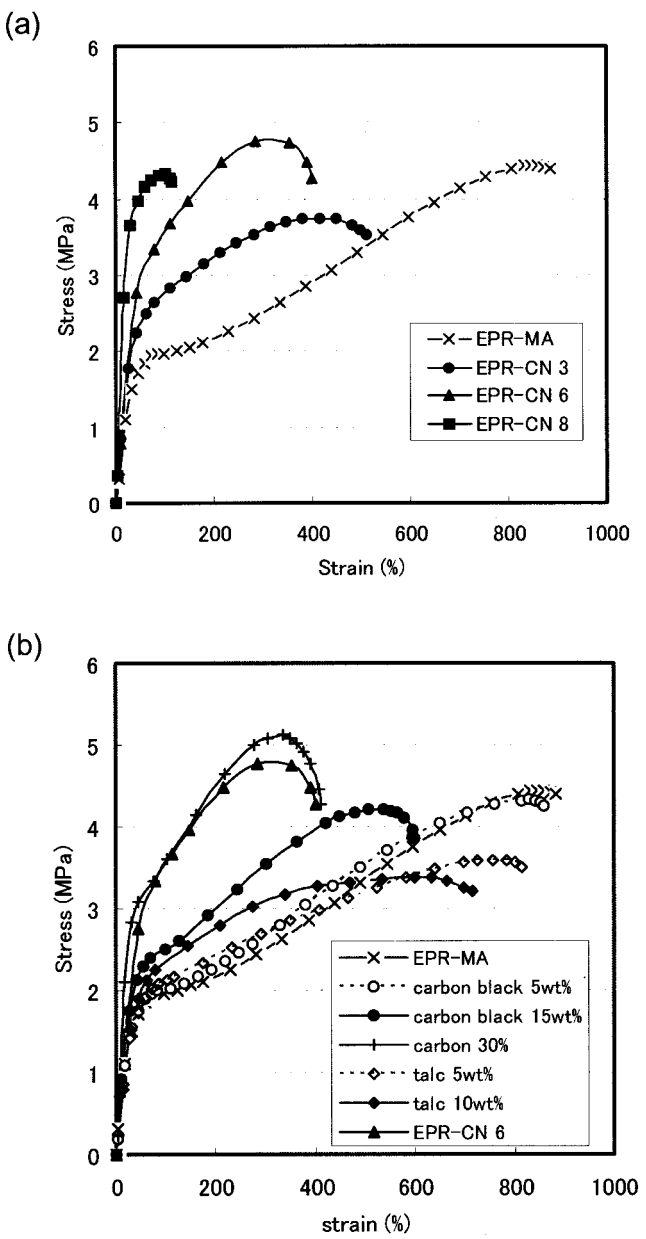

Figure 3 Representative stress–strain curves. (a) EPR-CNs; (b) Conventional composites.

TABLE I
Tensile Test Results

	Filler	Inorganic content (wt %)	Modulus (MPa)	Strength at maximum (MPa)	Elongation at break (%)
EPR-MA	—	0	7.2	4.4	900
EPR-CN 3	C18-Mt	2.9	11.2	3.7	550
EPR-CN 6	C18-Mt	6.1	17.2	4.7	400
EPR-CN 8	C18-Mt	8.3	23.2	4.2	130
Composite 1	Carbon black	5	7.9	4.3	860
2	Carbon black	15	12.8	4.2	600
3	Carbon black	30	18.0	4.8	400
4	Talc	4.9	7.1	3.6	820
5	Talc	10.1	7.5	3.4	720

EPR polymer chain is thought to be inhibited by the silicate layers dispersed at the nanometer level. The results of tensile tests are summarized at Table I. The tensile moduli of EPR–CNs increase with an increase of clay contents. The tensile modulus of EPR–CN 8 is three times higher than that of EPR-MA. The elongations of EPR–CNs at break decrease with the content of clay. It is thought that restriction of polymer chain rearrangement by dispersed silicate layers enhances the moduli of EPR–CNs but decreases the elongations at break of EPR–CNs. The tensile strengths at the first yields increase with the content of clay, as shown in Figure 1, due to the increase of the moduli. But for the tensile strength at the second yield point, EPR–CN 6 shows highest and EPR–CN 8 is lower than EPR–CN 6, because the elongation at break of EPR–CN 8 is extremely low. The strength at the second point of EPR–CN 3 is lower than EPR-MA. It is because restriction of polymer chain mobility by silicate layers is not enough in EPR–CN 3 and the elongation at break is smaller compared to EPR-MA.

Figure 3(b) shows the S-S curves of the conventional composites containing carbon black or talc in EPR-MA. The S-S curve of EPR–CN 6 is also shown for the comparison. Compared to the conventional composites with comparable amounts of the fillers loading (5 wt %), EPR–CNs 6 exhibit much higher modulus and much smaller elongation. The S-S curve of EPR–CN 6 is similar to that of the composite with 30 wt % carbon black loading. In the case of conventional composites, the first yield points in the S-S curves also become less pronounced and the elongations at break decreased with the content of carbon black.

Storage modulus

The temperature dependences of dynamic storage moduli of the samples are shown in Figure 4. The dynamic storage moduli of EPR–CNs are higher than those of EPR-MA in the range from −150 to 100°C. The relative storage moduli of EPR–CNs and the conventional composites to those of EPR-MA are shown in Figure 5. The relative storage moduli of EPR–CNs below glass transition temperatures (T_gs, around −35°C decided from the peak top of tanδ) are rela-

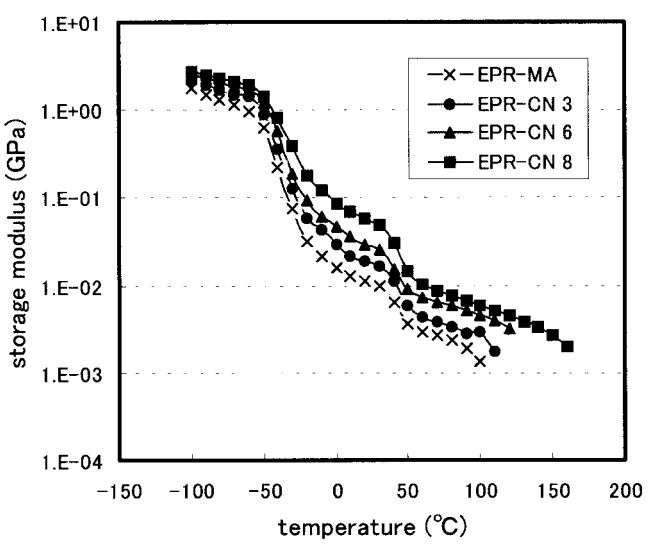

Figure 4 Storage moduli of EPR-CNs.

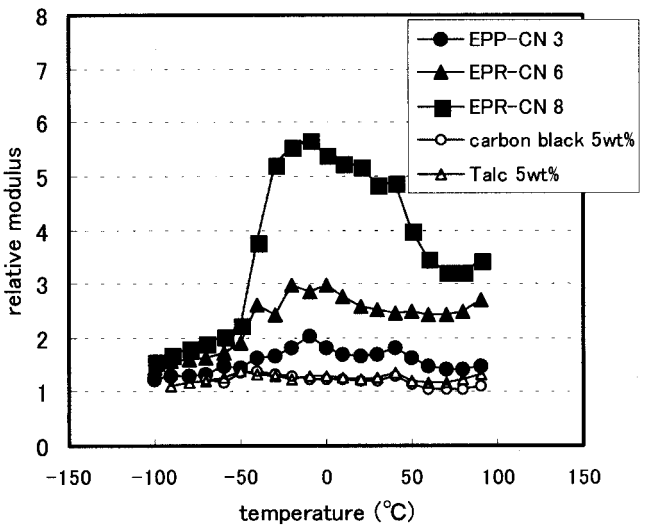

Figure 5 Relative storage moduli of EPR-CNs and conventional composites.

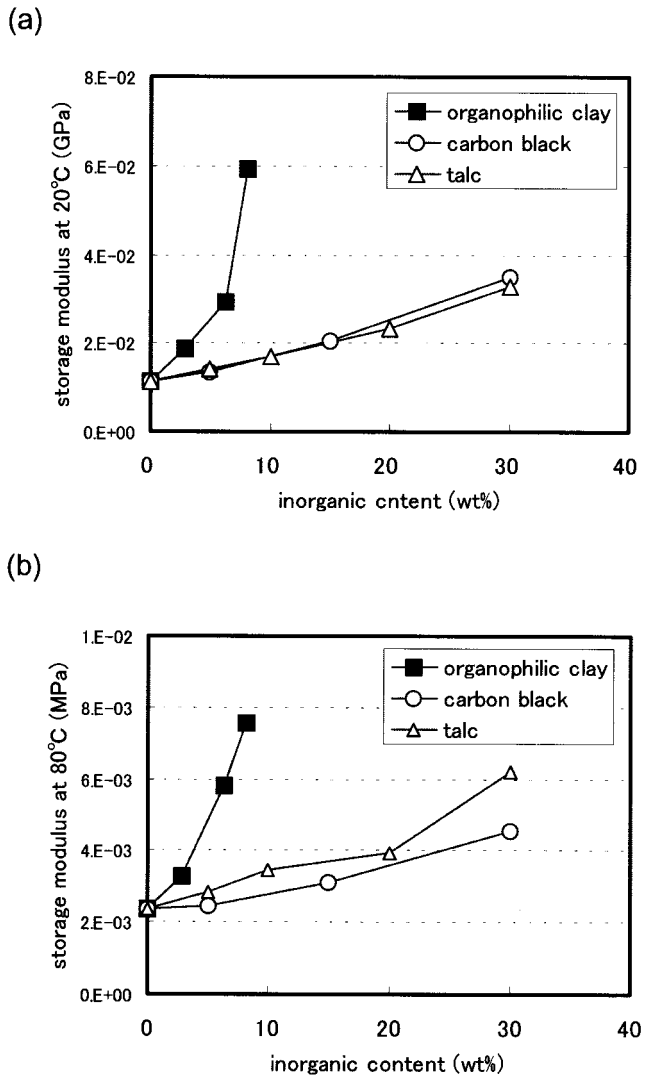

Figure 6 Storage moduli vs inorganic contents.

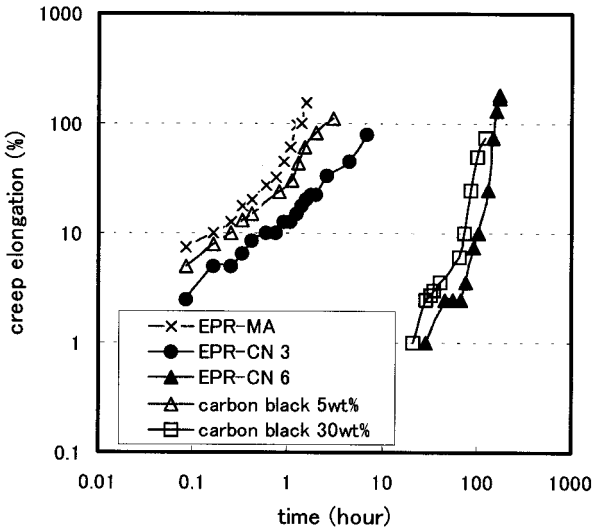

Figure 7 Creep test results.

tively small. They drastically increase above T_gs, go through the peak tops around −10°C and then decrease. The peak tops are observed between T_gs and melting points (around 45°C decided by differential scanning calorimeter) in EPR–CNs. The peak tops of relative storage moduli also appear in polymer–clay nanocomposites using crystalline polymer such as PP,[17,18] nylon 6 (unreported data). It is presumably because the crystallinity of the polymers at the interfaces with dispersed silicate layers might be different from that of the bulks of the polymers, and the melting points at the interfaces might be lower than those of the bulks. Further study to analysis the interface is in progress.

Figure 6 shows the relationships between the storage moduli and inorganic contents in EPR–CNs and the conventional composites at 20 and 80°C. The storage modulus of EPR–CN 6 at 20°C is comparable to those of the conventional composites with 30 wt % inorganic component loading [Fig. 6(a)]. It means that the organophilic clay dispersed at the nanometer level exhibit five times higher reinforcement effect compared for the conventional fillers. EPR–CNs also show approximately five times higher reinforcement effect at 80°C [Fig. 6(b)].

Creep property

The results of creep tests are shown in Figure 7. Creep elongations of EPR–CNs are remarkably smaller compared to EPR-MA. The elongation of EPR–CN 6 is restricted less than 1% at 30 h, while EPR-MA is elongated over 50% at 1 h and then is broken within 2 h. The composite with 5 wt % of carbon black do not exhibit remarkable enhancement in creep resistance, wherein it is elongated and is broken within 3 h. The composite with 30 wt % of carbon black shows enhancement in creep resistance, which is almost equal to EPR–CN 6. Figure 8 represents the schematic figure depicting the dispersed silicate layers and the EPR-MA polymer chains in EPR–CNs. It is thought that maleic anhydride groups (or maleic acid groups gen-

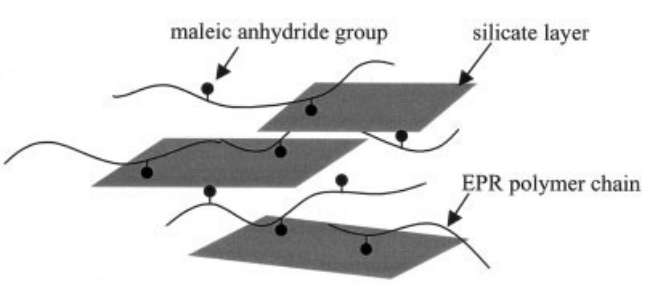

Figure 8 Schematic representations showing silicate layers and maleic anhydride modified EPR polymer chains.

erated by hydrolysis) grafted to the EPR polymer chains selectively absorb on the dispersed silicate layers and form strong ionic interaction, because maleic anhydrides have good affinity to ionic surfaces of the silicate layers. It is presumed that, as shown in Figure 8, the silicate layers dispersed at the nanometer level would be bridged with some polymer chains containing maleic anhydride groups. Thus, the dispersed silicate layers play a role of large pseudocrosslink points and improve creep resistance of EPR–CNs.

Swelling property

Figure 9(a)–(c) shows the increments in weight, in length on the plane, and in thickness of the samples (10 × 10 × 2 mm) soaked in hexadecane at 25°C, respectively. The swelling degrees of EPR–CNs were drastically restricted compared to EPR-MA. The weight increments of EPR–CNs decrease, as clay contents increase. The weight increment of EPR-MA is over 1700%, while that of the EPR–CN 8 is restricted to 333%. The length increments on the plane in EPR–CNs also remarkably become smaller with an increase of the clay contents. The length increment on the plane in EPR–CN 8 is restricted to 45% from 170% in EPR-MA. On the other hand, the thickness increments are barely restricted by organophilic clay loading. Figure 10 exhibits the swelling increments soaked after 1500 h vs inorganic contents in EPR–CNs and the conventional composites. The restricting effect in swelling by organophilic clay is remarkably superior to those by the conventional fillers, especially in weight and in length on the plane. The weight increment of EPR–CN 3 is approximately equal to those of the conventional composites with about 20 wt % conventional fillers loading. Figure 11 shows the anisotropy between the length increments on the plane and the thickness increments. EPR–CNs have a remarkable anisotropy between the length increments on the plane and the thickness increments, which is much higher than those in the conventional composites. The ratio in EPR–CN 8 is more than 2.5, while the conventional composites with less than 10 wt % fillers loading do not have anisotropies. It is known that not only polymer chains but also the dispersed silicate layers at the nanometer level are orientated in parallel with a sheet plane prepared by compression molding. It is thought that, by the orientations of both the silicate layers and the polymer chains, the swelling increment in the length on the plane is selectively restricted in EPR–CNs.

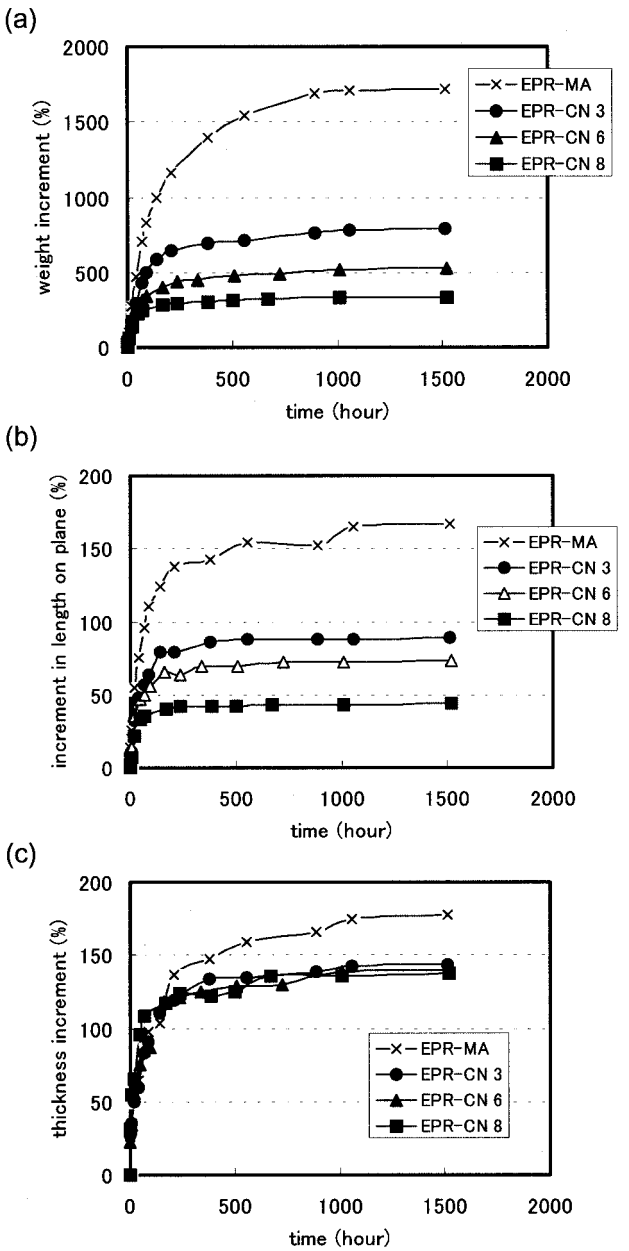

Figure 9 Swelling test results. (a) Weight increments; (b) length increments on plane; (c) thickness increments.

CONCLUSION

EPR–CNs were prepared by melt-compounding EPR-MA with C18-Mt, wherein the silicate layers exfoliated and dispersed into the nanometer level. Silicate layers dispersed at the nanometer level exhibit larger effect on the properties of EPR, such as mechanical, creep, and swelling properties, compared to comparable amounts of conventional fillers. It is because dispersed silicate layers have much larger interface with the EPR matrix and are thought to strongly restrain the EPR polymer chains. In application of thermoplastic elastomer for housing and automobiles, generally several kinds of fillers are loaded to satisfy multiple required properties. Clay nanocomposite technology is useful to improve properties of thermoplastic elastomer, because it is able to change their properties drastically with even a few percent silicate layers loading. Various kinds of thermoplastic elastomaers are expected to be produced by loading of silicate layers with or without conventional fillers.

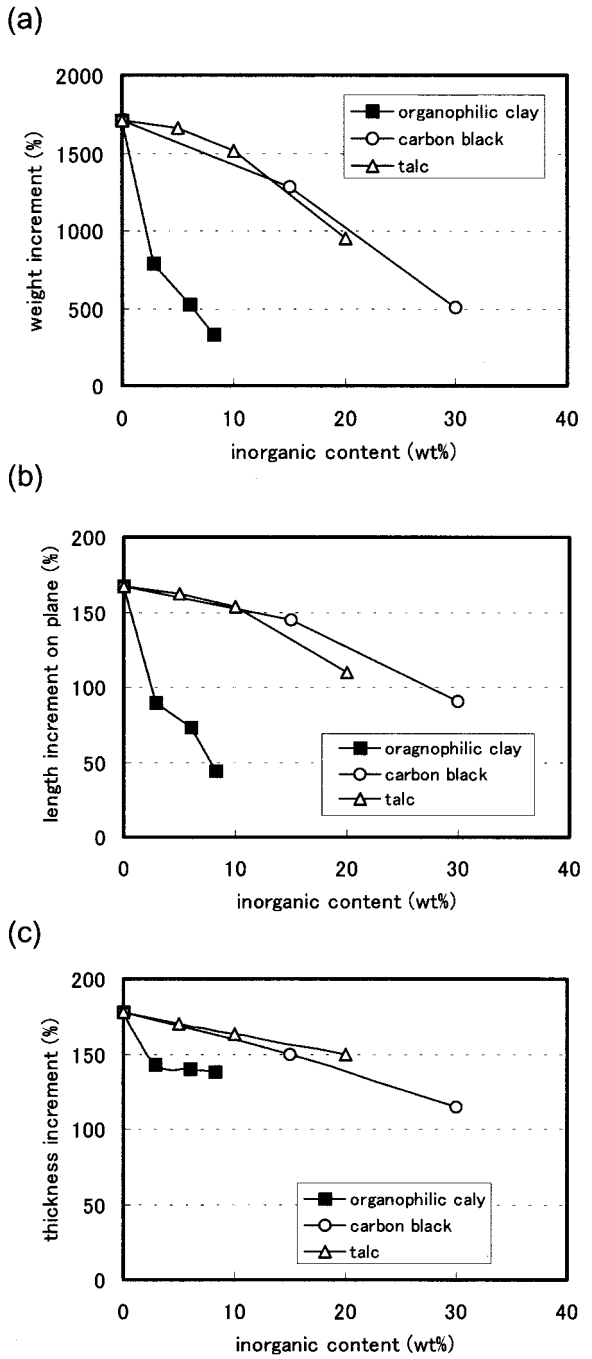

Figure 10 Swelling increments vs inorganic contents. (a) Weight increments; (b) length increments on plane; (c) thickness increments.

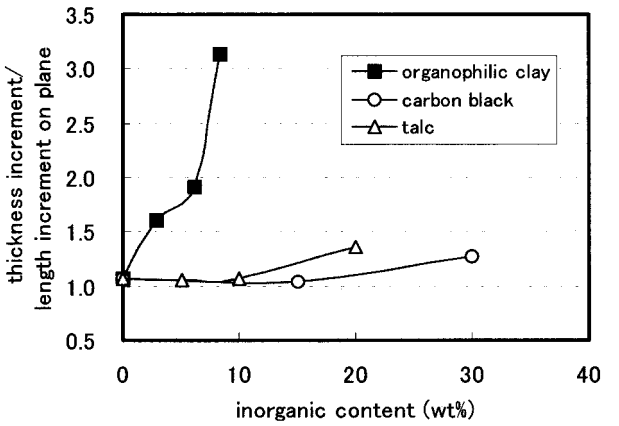

Figure 11 Anisotropy between length increments on length and thickness increments.

References

1. Schmidt, H. In Polymer Based Molecular Composites; Schaefer D. W.; Mark, J. E. Eds.; Material Research Society: Pittsburgh, 1990, p. 3.
2. Schmidt, H. K. Macromol Symp 1996, 101, 333.
3. Beecroft, L. L.; Ober, C. K. Chem Mater 1997, 9, 1302.
4. Usuki, A.; Kawasumi, M.; Kojima, Y.; Fukushima, Y.; Okada, A.; Kurauchi, T.; Kamigaito, O. J Mater Res 1993, 8, 1179.
5. Giannelis, E. P. Adv Mater 1996, 8 ,29.
6. Lagaly, G., Appl Clay Sci 1999, 15, 1.
7. LeBaron, P. C.; Wang, Z.; Pinnavaia, T. J., Appl Clay Sci 1999, 15, 11.
8. Yano, K.; Usuki, A.; Okada, A.; Kurauchi, T.; Kamigaito, O. J Polym Sci A Polym Chem 1993, 31, 2493.
9. Wang, M. S.; Pinnavaia, T. J. Chem Mater 1994, 6, 468.
10. Vaia, R. A.; Isii, H.; Giannelis, E. P. Chem Mater 1993, 5, 1694.
11. Moet, A.; Akelah, A. Mater Lett 1993, 18, 97.
12. Weiner, M. W.; Chen, H.; Giannelis, E. P.; Sogah, D. Y. J Am Chem Soc 1999, 122, 1615.
13. Hasegawa, N.; Okamoto, H.; Kawasumi, M.; Usuki, A. J Appl Polym Sci 1999, 74, 3359.
14. Biasci, L.; Aglietto, M.; Ruggeri, G.; Ciardelli, F. Polymer 1994, 35, 3296.
15. Kawasumi, M.; Hasegawa, N.; Kato, M.; Usuki, A.; Okada, A. Macromolecules 1997, 30, 6333.
16. Hasegawa, N.; Kawasumi, M.; Kato, M.; Usuki, A.; Okada, A. J Appl Polym Sci 1998, 67, 87.
17. Hasegawa, N.; Okamoto, H.; Kato, M.; Usuki, A. J Appl Polym Sci 2000, 78, 1918.
18. Hasegawa, N.; Okamoto, H.; Kawasumi, M.; Kato, M.; Tsukigase, A.; Usuki, A.; Macromol Mater Eng 2000, 280/281, 76.